

# Laser-optical characterization of the flow field behind the NGV cascade of a three-sector combustor simulator using filtered Rayleigh scattering

Michael Dues<sup>1\*</sup>, Ulrich Doll<sup>2</sup>, Tommaso Bacchi<sup>3</sup>, Alessio Picchi<sup>3</sup>, Guido Stockhausen<sup>4</sup>, Christian Willert<sup>4</sup>

<sup>1</sup> ILA R&D GmbH, Jülich, Germany

<sup>2</sup> Paul Scherrer Institute, 5232 Villigen PSI, Switzerland

<sup>3</sup> Università degli Studi di Firenze (UNIFI), 50139 Firenze, Italy

<sup>4</sup> Institute of Propulsion Technology, German Aerospace Centre (DLR), 51170 Köln, Germany

\* Correspondent author: dues@ila.de

**Keywords** filtered Rayleigh scattering, turbine flow, temperature, pressure, flow velocity, Doppler shift

## ABSTRACT

The aero-thermal properties of the flow field downstream of an NGV cascade of a three-sector combustor simulator rig are characterized by means of five-hole probe/ temperature sensor measurements as well as laser-optical FSM-FRS diagnostics. Both methods are applied to acquire and analyze pressure, temperature and velocity information in a cross section downstream of the NGV. The study discusses current capabilities as well as limitations of both methods when being applied to turbomachinery configurations. In general, results obtained with both methods are on a similar absolute level. Based on a more detailed analysis, strong evidence for an intrusive interaction between the five-hole probe and the flow downstream of the NGV is found, which is significantly influencing the probe's measurement accuracies.

---

## 1. Introduction

With the introduction of modern lean burn aero-engine combustors, enhanced distortions are introduced at the turbine inlet plane. As a consequence of novel injector designs and the redirection of air mass, highly swirling flows, characterized by severe temperature gradients (hot streaks) and relevant turbulence, approach the turbine. These unsteady flow fields significantly challenge the reliability of common design procedures (Chevrier & Bertrand, 2017; von der Bank et al, 2014). Within this framework, a three-sector rig made up of a combustor simulator and a nozzle guide vane (NGV) cascade was installed at THT Lab (Laboratory of Technologies for High Temperature) of University of Florence. In the combustor simulator, representative temperature distortions swirl and turbulence fields are generated through the mixing of a heated main flow, passing through three axial swirlers, and liner cooling flows at ambient temperature

(Bacci et al, 2015). The focus of the present study lies on the experimental characterization of pressure, temperature and velocity distributions downstream of the nozzle guide vane cascade.

In order to acquire this kind of data, conventional measurement devices such as five-hole probes with additional temperature sensors are commonly used because they are well proven and their uncertainty budget is well understood (Heinke et al, 2004; Luque et al, 2015; Qureshi et al, 2012). But these techniques also have disadvantages: Foremost, due to their invasive nature, they disturb the flow field at the actual measurement position, which is especially critical in narrow flow channels typically found in turbomachinery applications (Aschenbruck et al, 2015; Sanders et al, 2017). In addition, these probes are limited in terms of spatial resolution and temperature range and they cannot easily be applied to rotating systems. Therefore the development of optical methods for the investigation of flow fields in turbomachines is still an important task.

The optical measurement of velocity fields by PIV has improved a lot over the past 20 years and thus PIV became a standard tool in experimental fluid mechanics. Comparable techniques with respect to usability and reliability to assess temperature or pressure distributions did not evolve. State-of-the-art laser-optical temperature measurement techniques like CARS and Raman scattering are capable of yielding accurate unsteady temperature measurements. Their drawback lies in the necessity of complex hardware in form of powerful pulse laser systems and they are limited to point measurements. Laser Rayleigh scattering can in principle be used to acquire two-dimensional temperature data, but due to its susceptibility to background scattering, the technique cannot be applied to characterize internal flows.

The successful implementation of the filtered Rayleigh scattering technique (FRS) (Miles & Lempert, 1990), extended by the method of frequency scanning (FSM-FRS) (Doll et al, 2014; Forkey, 1996) at DLR Cologne over the past years might prove a useful contribution for the investigation of flow fields because

- FSM-FRS can use the same optical access used for PIV-Measurements. Therefore it is easy to apply to most existing test rigs.
- FSM-FRS does not need tracer particles to be added to the flow, which might be important for flows with high circumferential components or cryogenic applications.
- FSM-FRS can be used close to surfaces because laser light reflections are strongly attenuated by molecular filtering.
- FSM-FRS is capable to measure time-averaged planar three-component velocity, pressure and temperature distributions simultaneously (Doll et al, 2017).

- The uncertainty budget was investigated in detail and methods are developed to decrease measurement uncertainties to relative values  $\sim 1\%$  (Doll et al, 2016).
- FSM-FRS delivers spatially resolved quantitative multi-parameter measurement data, which can be used e. g. for the validation of CFD calculations.

In this contribution, the FSM-FRS technique is used to investigate pressure, temperature and velocity fields behind the NGV of a three-sector gas turbine combustor simulator. FSM-FRS measurement results are compared against conventionally measured data acquired by means of a five-hole probe equipped with an additional thermocouple sensor.

## 2. Principle of FSM-FRS

The FRS technique relies on the filtering of laser stray light from surfaces or windows by means of molecular absorption and is thus well suited to characterize internal flows. The principle of FRS is illustrated in Fig. 1: Due to broadening mechanisms related to molecular motion, the Rayleigh scattering's spectral width totals several GHz, while scattering from surfaces (geometric) or Mie scattering from large particles has the same linewidth as the incident laser light. If now a molecular filter is placed in front of the detector, the narrow linewidth scattering is strongly attenuated while portions of Rayleigh scattering pass through the molecular filter. These portions hold information on pressure, temperature and flow velocity inside the investigated volume.

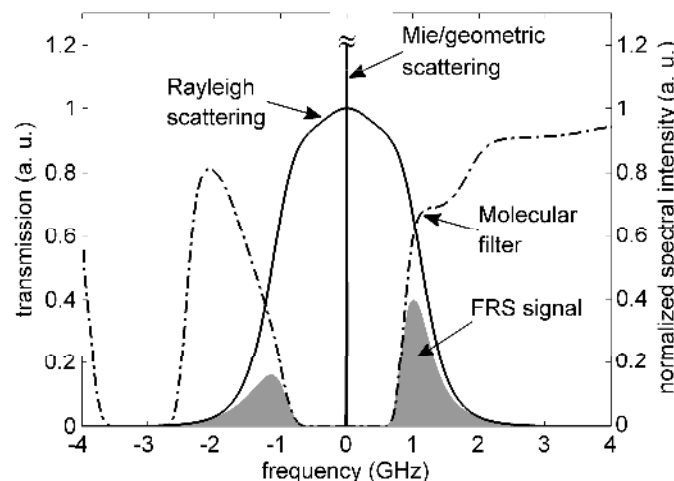


**Fig. 1:** Narrow linewidth laser light scattering is strongly attenuated by the molecular filter, while portions of Rayleigh scattering pass through.

As typically CCD technology is used to record the scattered intensity, spectral details on the measured quantities are lost due to on-chip integration. The frequency scanning method offers a viable solution to restore the spectral information. As indicated in Fig. 2, in FSM-FRS the laser's output frequency is tuned in discrete steps along the molecular filter's absorption profile. In acquiring images at each frequency step, intensity spectra at each sensor element are gathered. These intensity spectra can then be used to simultaneously retrieve pressure, temperature and velocity maps.

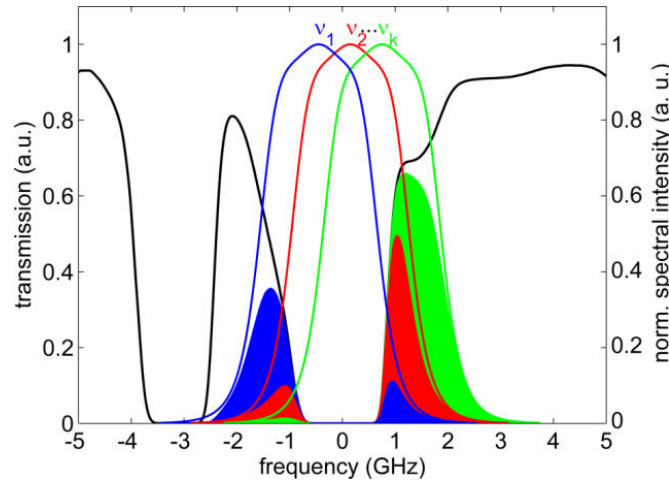


**Fig. 1:** Frequency scanning method: The laser's output frequency is modulated multiple times along the molecular filter's transmission profile.

### 3. Set up of the test rig and of the measurement systems

The experimental survey was carried out on a test rig made of a non-reactive, three-sector combustor simulator coupled with a high pressure NGV cascade. Sectional views of the test rig's CAD model are reported in Fig. 3. Red and blue arrows have been sketched in order to allow a better understanding of the flow field evolution. The mainstream is heated up to 423 K and passes through three axial swirlers, which create a highly swirling flow in the chamber. Two separate lines, at ambient temperature, feed the effusion cooled inner and outer liner. The interaction between the three flows generates a lean burn combustor representative flow field at the combustor exit. Relevant temperature distortions, together with high degree of swirl ( $\pm 50^\circ$ ) and turbulence intensity (up to  $\approx 30\%$ ) are achieved on Plane 40, nominally the combustor-turbine interface plane. The combustor simulator presents typical features of modern lean burn combustors in form of main-coolant mass flow split (65%-35%), effusion cooled liners without dilution holes, and limited axial dimensions ( $\approx 2.5$  swirler diameters). The three sector configuration was chosen in order to make the central sector flow field, target of all the measurements, insensitive to the presence of the rig lateral walls. Ducts of 55mm length (35% of

the chamber length) are installed on the swirlers in order to postpone the swirling structure expansion and its interaction with liner cooling flows and, therefore, achieve enhanced temperature and flow distortions at the chamber exit. The temperature field achieved on the central sector of Plane 40, measured by probe traversing within a preliminary investigation, is reported in Fig. 4, observed in downstream direction; the boundaries of the central sector are reported as well. A clear hot streak in the annulus center can be recognized, with a maximum-to-minimum temperature ratio that reaches about 1.2. The wavy shape of the hot spot is due to the clockwise swirling flow that bleeds liner coolant towards the mean radius.

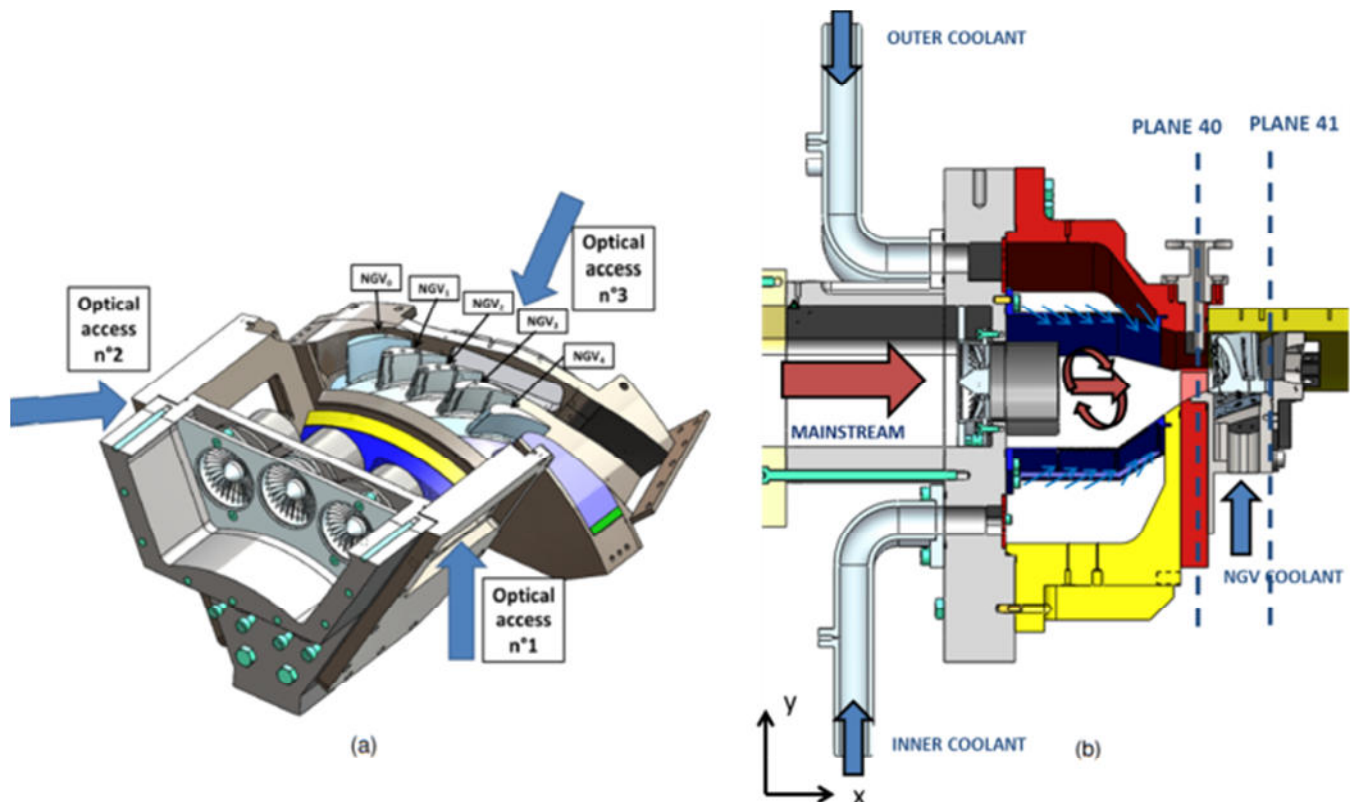


**Fig. 2:** Sectional views of the test rig's CAD model

The NGV cascade is made by five vanes – six passages, in order to reach a swirler-to-vane count ratio of 1:2. The central vane has the leading edge aligned with the central swirler. Since only the central sector (i.e. two vane pitches) is subject of the investigation, only the three central airfoils (NGV1-2 in Fig. 3a) are film-cooled. Two dummy airfoils (NGV0 and NGV4) have been installed at their sides. The NGV cooling flow is provided by a further line at ambient temperature. A back-pressure valve is used to regulate the rig pressurization: a chamber pressure of 148 kPa and an average Mach number at the cascade exit of 0.64 (in the presence of film-cooling flows), are achieved in the nominal operating point.

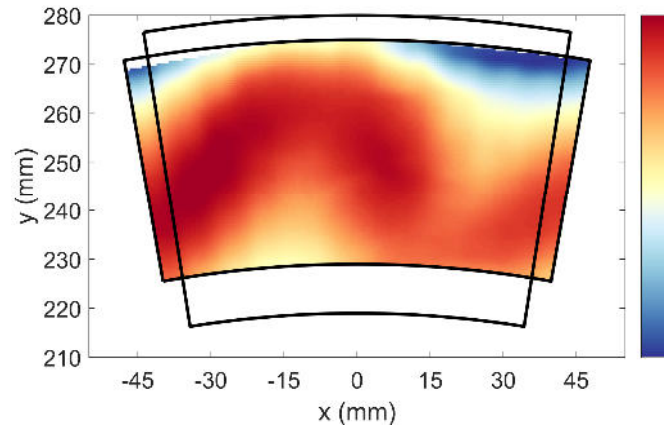


**Fig. 3:** Probe measurement of the static temperature map on Plane 40

The test rig is provided with different kinds of accesses to support the adopted measurement techniques. Two adaptive flanges are located upstream and downstream of the cascade (Plane 40 and Plane 41), in order to carry out probe traversing on these planes. Plane 40 is located half an axial chord upstream of the vane leading edge, while Plane 41 is about 0.25 axial chords downstream of the vane trailing edge. The upstream flange is easily recognizable in Fig. 3b. The rig is also provided with three optical accesses (Fig. 3a), to be exploited for optical measurements on the vane profiles and downstream of them. Only the third one of them, realized in the exit duct, was used in the present investigation, in order to observe Plane 41 from downstream direction.

### 3.1 Probe traversing set-up

Probe measurements have been carried out by means of a five hole probe equipped with a J-thermocouple. A *Vectoflow*<sup>®</sup> cobra-shaped five hole probe was used, with a 3mm head. The thermocouple is installed above the probe head, inside a shroud, as for a Kiel probe, in order to make the thermocouple recovery factor more insensitive to high flow angles and reduce the measurement uncertainty. A traverse system, installed on the above described flanges, was used to automatically drive the probe within the measurement planes. On Plane 41, a 335 points measurement mesh was used. Radial and tangential resolutions of about 2.5mm and 1° were achieved, resulting in about 10 points per each NGV pitch. Due the probe dimensions it was not possible to investigate the annulus areas in the very proximity of the end walls: the investigated domain covers from 7 to 82% of the radial span. For each mesh point, data were acquired and averaged over a 2 seconds sampling time. A 2 seconds stand-by interval was set, between the

instant when the probe reached the measurement position and the start of the acquisition. In order to characterize the probe recovery factor, a thorough calibration process was carried out; yaw angles up to  $\pm 75^\circ$  and pitch angles up to  $+75^\circ/-60^\circ$ , where investigated, while a set of Mach numbers were imposed up to 0.9. The temperature measurement uncertainty stays below 2% of the reading, within the measured range of Mach numbers and flow angles.

### 3.2 FSM-FRS set-up

In Fig. 5 a schematic of the FSM-FRS systems components is depicted. The system is founded on a Coherent Verdi V5 continuous wave laser, emitting single-frequency light at 532 nm with an output power of up to 5 W and a linewidth  $<5$  MHz. The laser's frequency can be modified by heating or cooling an intra-cavity etalon as well as by issuing control voltages on two piezoelectric elements and thus altering the resonator's length.

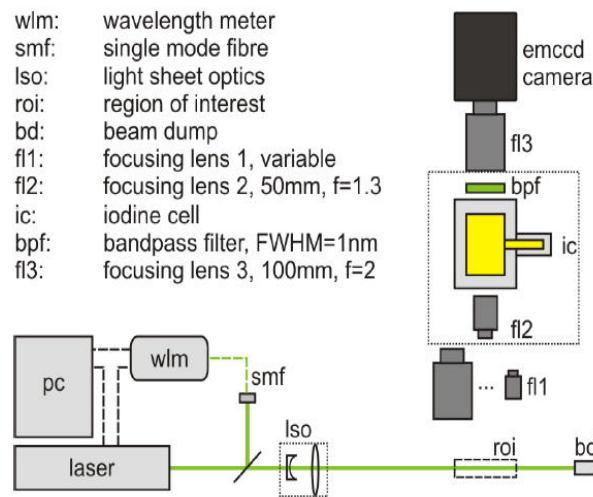


**Fig. 4:** Components of the FSM-FRS system

The laser's output frequency is monitored and actively controlled by a High Finesse WSU 10 wavelength meter, which has an absolute accuracy of 10 MHz and enables, by issuing a control voltage on one of the piezos, a relative stability of the laser's output frequency below 2 MHz of the setpoint. A second control loop accounts for thermal effects in the laser's resonator and ensures long-term frequency stability.

Light scattered from the plane of interest is collected by a first camera lens and enters the transfer optics, which is composed of two additional lenses in retro position. In between, a

molecular iodine filter cell as well as a bandpass filter (Barr, FWHM 1 nm) is placed. Light exiting the filter array is accumulated by a Hamamatsu C9100-13 EM-CCD camera.

Laser illumination at Plane 41 was realized by utilizing the flange, which was originally designed for probe traversing, by equipping it with a window. The laser beam was brought in from above by means of an articulated mirror arm (ILA) and formed into a collimated light sheet of 45 mm width by means of an optical scanner arrangement. To cover the whole visible area with laser light, the sheet optics was traversed once in lateral direction. As indicated in Fig. 3, Plane 41 is observed through optical access No. 3. To minimize obstructions of the flow channel due to geometrical restrictions the detection unit was positioned under an angle of  $21^\circ$  with respect to the rig axis.

#### 4. Results

Velocity measurements by FRS are based on the optical Doppler shift. For a given scattering geometry, an observer registers a frequency shift which is proportional to the projection of the flow velocity onto the bisector spanned by laser direction and observer position. As in this study only a single camera view was used, a 3-component velocity vector cannot be reconstructed from such a measurement. Therefore, in order to realize a direct comparison between velocity information gathered by FSM-FRS against five-hole probe data, five-hole probe velocity results were transformed into Doppler frequency shifts

In Fig. 7 a comparison of pressure, temperature and Doppler shift maps measured with FSM-FRS and interpolated from five-hole probe data is shown. Caused by the size and geometry of the five-hole probe on the one hand and the limited optical access for FSM-FRS on the other, the measurement area feasible for both methods is limited and marked by dashed lines. The positions of the NGV blade's trailing edges are drawn as dotted lines.

Pressure distributions obtained by FSM-FRS and five-hole probe are on a similar absolute level of about 1100 hPa. But the data quality of the FSM-FRS data set was not sufficient to calculate a reasonable pressure distribution. The reason may lie in an insufficient correction of laser induced background light, which is caused by strong reflection of the laser light sheet at the NGVs airfoils.



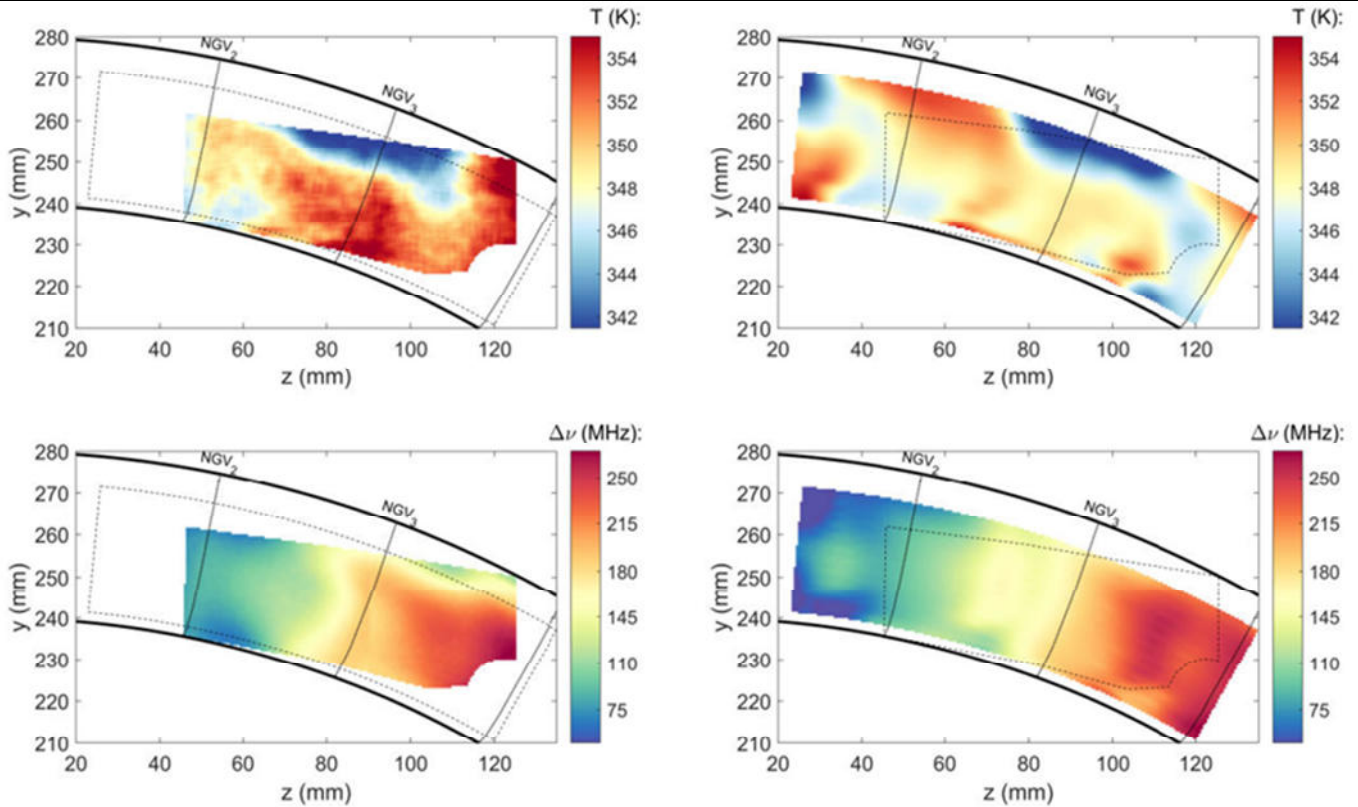


**Fig. 7:** Comparison of temperature (top) and Doppler shift (bottom) maps measured with FRS (left) and interpolated probe data (right). Black dashed lines mark respective areas covered by FRS and probe measurements, black solid lines mark the channel boundaries.

The temperature distributions for both methods represent a good agreement in topology and level. Five-hole probe and FSM-FRS data detect a cold streak starting from the outer casing between NGV2 and NGV3 and extending into the area in-between NGV3 and NGV4. However, only the probe measurements display a propagation of the cold streak towards the inner casing, while the FSM-FRS system detects higher temperatures about 5K in the centre of the flow channel. A cold spot at the lower end of NGV2 is visible in both data sets.

Doppler frequency shifts measured by FSM-FRS and calculated from five-hole probe velocity data in general exhibit similar structures as well as absolute level. However, while FSM-FRS measurements detect a sharp gradient in the Doppler frequencies upstream of NGV3, this area appears blurred in the five-hole probe data.

A more detailed view on the differences in Doppler shift is offered by Fig. 8. The Doppler frequency shift of both data sets is displayed for a radial profile near centreline of the flow channel. Red transparent zones mark the wake regions corresponding to the respective NGV

vane to the left. Wake position and dimensions are estimated using empiric formulas (Ainley & Mathieson, 1951; Lakshminarayana & Davino, 1980).

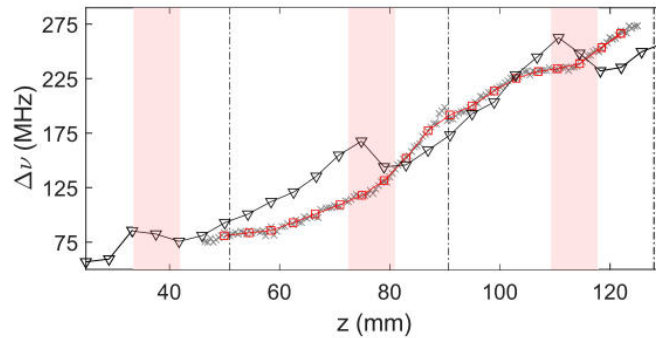


**Fig. 8:** Radial centreline profile of the Doppler frequency-shift for FSM-FRS (gray,  $\times$ ) and five-hole probe (black,  $\nabla$ ) measurement results. Red lines represent FSM-FRS results mapped onto the five-hole probe measurement grid. Dashed-dotted lines mark NGV trailing edge positions projected onto the measurement plane, red transparent areas indicate respective wake regions.

While the Doppler frequency shifts measured by FSM-FRS increase continuously along the circumferential position  $z$ , Doppler shifts calculated from probe data steadily grow with differing slope in the passages in-between two airfoil wakes. This is followed by a steep drop inside the actual wake area. The sudden drop of five-hole probe Doppler shifts inside the airfoils' wake regions is probably associated with erroneous probe readings caused by strong pressure gradients present in these zones (Aschenbruck et al, 2015; Hoenen et al, 2012; Sanders et al, 2017). In addition, local differences between five-hole probe data and FSM-FRS results in the passages might be related to an intrusive impact of the probe body on the flow. As can be seen from Fig. 9, size of probe head and stem are not negligible compared to the size of the NGV passages, which may lead to a substantial blockage of the actual flow channel.

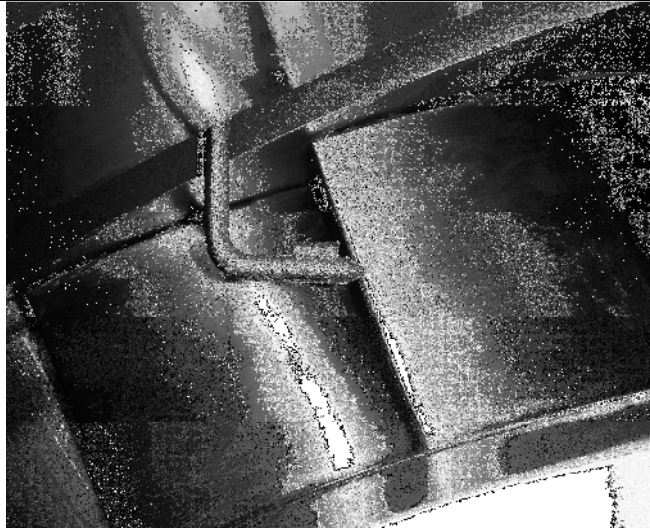


**Fig. 9:** Dimension and arrangement of the five hole probe inside the flow channel.

## 5. Conclusion

Conventional five-hole probe/temperature sensor measurements as well as laser optical FSM-FRS measurements were applied to investigate the aerothermal flow properties inside a test rig made-up of a non-reactive, three-sector combustor simulator combined with a high pressure NGV cascade. The study discusses current capabilities as well as limitations of both methods when being applied to turbomachinery configurations.

In general, both measurement methods indicate comparable level and distributions of temperature and velocity information. Due to a detailed analysis of the differences between FSM-FRS and five-hole probe datasets an interaction of the probe head with the flow field can be assumed, resulting in false velocity readings inside the airfoil wakes by the probe as well as in a significant blocking impact on the passage flows downstream of the NGV cascade. Future FSM-FRS measurements with more camera positions could provide velocity vector maps combined with temperature and pressure information to investigate this influence in detail.

Comparing both measurement methods, the probe technology provides a well proven tool with high accuracy for the investigation of temperature and velocity fields. The spatial resolution of the measurement is limited by the probe head's dimensions as well as by the number of measurement points realized by the probe traverse. For turbomachinery applications a possible interaction of the probe with flow structures like wakes, vortices and boundary layers should be taken into account. A measurement inside rotating cascades is very difficult. In the current configuration, measurement area and the available velocity information of FSM-FRS are limited

due to the optical accessibility. The remarkable spatial resolution is only limited by the camera resolution. Because the method is non-intrusive, the flow field itself is not influenced by the measurement. As a future aspect even the application in rotating cascades at elevated temperature and pressure levels should be feasible.

## Acknowledgment

The authors wish to gratefully acknowledge FACTOR (Full Aerothermal Combustor-Turbine interactions Research) Consortium for the kind permission of publishing the results herein. FACTOR is a Collaborative Project co-funded by the European Commission within the Seventh Framework Programme (2010-2016) under the Grant Agreement no. 265985.

## References

- Ainley, D. G. & Mathieson, G. C. R. (1951) *A Method of Performance Estimation for Axial-flow Turbines* H.M. Stationery Office.
- Aschenbruck, J., Hauptmann, T. & Seume, J. R. (2015) Influence of a multi-hole pressure probe on the flow field in axial-turbines, *11th European Conference on Turbomachinery Fluid Dynamics and Thermodynamics, ETC 2015*.
- Bacci, T., Cacioli, G., Facchini, B., Tarchi, L., Koupper, C. & Champion, J.-L. (2015) Flowfield and Temperature Profiles Measurements on a Combustor Simulator Dedicated to Hot Streaks Generation, *ASME Turbo Expo 2015: Turbine Technical Conference and Exposition*.
- Chevrier, M. & Bertrand, H. (2017) *Full Aero-thermal Combustor-Turbine interactiOn Research (FACTOR) - Final Publishable Summary Report*.
- Doll, U., Burow, E., Stockhausen, G. & Willert, C. (2016) Methods to improve pressure, temperature and velocity accuracies of filtered Rayleigh scattering measurements in gaseous flows. *Measurement Science and Technology*, 27(12), 125204-125204.
- Doll, U., Stockhausen, G. & Willert, C. (2014) Endoscopic filtered Rayleigh scattering for the analysis of ducted gas flows. *Experiments in Fluids*, 55(3), 1-13.
- Doll, U., Stockhausen, G. & Willert, C. (2017) Pressure, temperature, and three-component velocity fields by filtered Rayleigh scattering velocimetry. *Opt. Lett.*, 42(19), 3773-3776.
- Forkey, J. (1996) *Development and Demonstration of Filtered Rayleigh Scattering: a Laser Based Flow Diagnostic for Planar Measurement of Velocity, Temperature and Pressure* Princeton University.

Heinke, W., König, S., Matyschok, B., Stoffel, B., Fiala, A. & Heinig, K. (2004) Experimental investigations on steady wake effects in a high-lift turbine cascade. *Experiments in Fluids*, 37(4), 488-496.

Hoenen, H. T., Kunte, R., Waniczek, P. & Jeschke, P. (2012) Measuring Failures and Correction Methods for Pneumatic Multi-Hole Probes, *ASME Turbo Expo 2012: Turbine Technical Conference and Exposition*.

Lakshminarayana, B. & Davino, R. (1980) Mean Velocity and Decay Characteristics of the Guidevane and Stator Blade Wake of an Axial Flow Compressor. *Journal of Engineering for Power*, 102(1), 50-60.

Luque, S., Kanjirakkad, V., Aslanidou, I., Lubbock, R., Rosic, B. & Uchida, S. (2015) A New Experimental Facility to Investigate Combustor-Turbine Interactions in Gas Turbines With Multiple Can Combustors. *Journal of Engineering for Gas Turbines and Power*, 137(5).

Miles, R. & Lempert, W. (1990) Two-dimensional measurement of density, velocity, and temperature in turbulent high-speed air flows by UV Rayleigh scattering. *Applied Physics B: Lasers and Optics*, 51, 1-7.

Qureshi, I., Smith, A. D. & Povey, T. (2012) HP Vane Aerodynamics and Heat Transfer in the Presence of Aggressive Inlet Swirl. *Journal of Turbomachinery*, 135(2), 021040--021040-13-021040.

Sanders, C., Terstegen, M., Hölle, M., Jeschke, P., Schönenborn, H. & Fröbel, T. (2017) Numerical Studies on the Intrusive Influence of a Five-Hole Pressure Probe in a High-Speed Axial Compressor, *ASME Turbo Expo 2017: Turbomachinery Technical Conference and Exposition*.

von der Bank, R., Donnerhack, S., Rae, A., Cazalens, M., Lundblad, A. & Dietz, M. (2014) LEMCOTEC: Improving the Core-Engine Thermal Efficiency, *ASME Turbo Expo 2014: Turbine Technical Conference and Exposition*.